NASA Technical Memorandum 81154

Flight Test of Navigation and Guidance Sensor Errors Measured on STOL Approaches

David N. Warner, Jr. and F. J. Moran

December 1979

National Aeronautics and Space Administration

NASA Technical Memorandum 81154

Flight Test of Navigation and Guidance Sensor Errors Measured on STOL Approaches

David N. Warner, Jr.
F. J. Moran, Ames Research Center, Moffett Field, California

National Aeronautics and
Space Administration

Ames Research Center
Moffett Field, California 94035

TABLE OF CONTENTS

ABBREVIATIONS AND SYMBOLS

A_{b_1}, A_{b_2}, A_{b_3}	accelerations measured with respect to aircraft body axes
A_{R_1}, A_{R_2}, A_{R_3}	accelerations measured with respect to runway axes
A_{S_1}, A_{S_2}, A_{S_3}	accelerations measured with respect to INS sensing axes
b_1, b_2, b_3	aircraft body axes
dt	time interval for dV
dV	change in velocity (integral of INS accelerations)
g	gravitational constant
N, E, D	north, east, down axes system
P_1, P_2, P_3	axes system orienting INS with respect to NED through wander angle ψ_w
R_1, R_2, R_3	runway axes system; R_1 is longitudinal axis
S_1, S_2, S_3	axes systems of INS about which INS accelerations are measured
STOL	short takeoff and landing
t	time on plot
X, Y, Z	aircraft position in runway coordinates
θ	pitch angle
ϕ	roll angle
ψ	yaw angle of aircraft with respect to north
ψ_E	$\psi - \psi_{R/N}$
$\psi_{R/N}$	angle of runway axis with respect to north
$\psi_{S/R}$	angle of runway axis with respect to INS longitudinal axis

ψ_w	wander angle of INS platform
σ	standard deviation

FLIGHT TEST OF NAVIGATION AND GUIDANCE SENSOR ERRORS MEASURED ON STOL APPROACHES

David N. Warner, Jr. and F. J. Moran

Ames Research Center

SUMMARY

Navigation and guidance sensor error characteristics have been measured during STOL approach-flight investigations. Data from some of the state sensors of a digital avionics system have been compared to corresponding outputs from an inertial navigation system. These sensors include the vertical gyro, compass, and accelerometers. Barometric altimeter data were compared to altitude measured by a tracking radar. Data were recorded with the Augmentor Wing Jet STOL Research Aircraft parked and in flight.

INTRODUCTION

The accuracy of aircraft navigation, guidance, and control systems depends heavily on the interrelationships between the trajectories flown and the error characteristics of the sensors used by those systems. Some standard aircraft sensors which are commonly used with advanced avionics systems include a vertical gyro, compass, 3-axis accelerometers, and a barometric altimeter. The major error characteristics of the instruments are generally well known and have been described in texts, such as reference 1. However, error characteristics which are acceptable in conventional takeoff and landing (CTOL) navigation, guidance, and control systems may pose problems when used in short takeoff and landing (STOL) systems. Sensor errors in flights with short final approach distances and high glide-slope angles, for instance, have had very limited coverage in the literature and may also adversely affect navigation, guidance, and control systems performance, as indicated in references 2, 3, and 4.

This report describes a STOL aircraft flight test and data analysis which compared outputs from the vertical gyro, accelerometers, compass, and altimeter to similar outputs from an inertial navigation system and a tracking radar system. Data are presented which show the predominate sensor errors, both static and maneuver-induced. The information presented should be useful in the design of navigation, guidance, and control systems, and in analysis of test results.

A Litton LTN-51 inertial navigation system (INS) was installed in the Augmentor Wing Jet STOL Research Aircraft (fig. 1) and interfaced to the data recorder and to the digital avionics system (ref. 2). During the tests at NASA's facility at NALF Crows Landing, California, data from both the INS and the airborne instruments were telemetered to a ground data facility. Aircraft

position data from a tracking radar was time correlated and merged with the airborne data, and recorded for later analysis. Data were recorded as the aircraft was parked on the ramp and during flight. The flight data to be reported were taken during the initial climb, the turn and flight downwind, turn to final, approach on a 7° glide slope, and the landing. The data were analyzed to compute the sensor errors relative to the INS and radar references.

TEST PROCEDURES

Inertial Navigation System

The roll, pitch, heading, and acceleration reference signals were measured by a Litton LTN-51 INS. This INS meets or exceeds the requirements documented in the Aeronautical Radio Inc. (ARINC) Characteristic No. 561-5 (ref. 4). The specifications for the roll, pitch, heading, and platform wander angle signals from the INS are documented in appendix A. The analog accelerometer signals from the INS were digitized in interface equipment described below. Specifications for these signals are also included in appendix A.

The basic function of the digitizer interface unit is to integrate accelerations along three independent axes. The outputs are 12-bit digital words (with proper sign) which represent the result of the integration of acceleration over an interval dt in each of these axes. The integral, or change in velocity dV is over an accurately controlled interval of time dt, after which the three dV appear in separate holding registers awaiting parallel transfer to the avionics system digital computer. This digitizing process was used instead of standard analog to digital converters to provide proper impedance matching between the INS and the avionics system.

Tracking Radar

The aircraft position relative to the test facility coordinate system was measured by a tracking radar. The coordinate system and the test facility are shown in figure 2. The radar altitude, measurement Z, was the reference for computing errors in the barometric altitude. Accuracy of the radar is shown in table 1 and documented more fully in appendix A of reference 5. The maximum error in the radar Z measurement during the test flight was approximately 4 m based on the elevation and range accuracy in table 1.

Flightpath

Data were recorded from all test and reference sensors as the airplane was (1) parked on the ramp, and (2) flown around a typical experiment test pattern. Data were taken during the climb to altitude, left turn, flight downwind, turn to final, approach on 7° glide slope, and landing on the marked STOLport. The path as measured by the tracking radar is shown in figure 3(a). The X, Y, altitude, and heading measurements as a function of time are shown in figure 3(b). Final approach on the 7° glide slope started about 1 min

prior to touchdown at a range of 2200 m (1.2 n. mi.). Final approach speed was 68 knots.

DISCUSSION AND TEST RESULTS

A brief description of each of the airborne sensors and a discussion of the test results will be presented in this section. The sensors are the vertical gyro, compass, accelerometers, and barometric altimeter.

Vertical Gyro

Description

A Sperry Flight Systems vertical gyro provides pitch- and roll-attitude data to the onboard digital avionics system. The gyro is a non-restrained, two gimbal, electrically driven displacement gyro. Sine-cosine synchro signals from the vertical gyro are digitized for input to the avionics system computer. The Euler angles conversion occurs in the computer. Resolution of the pitch and roll angles in the software computations is 0.00278°/count. Specifications on the vertical gyro are in appendix A.

After power is applied to the vertical gyro, fast and slow erection circuits stabilize the gyro within 1.5 to 2 min. The erection system uses electrolytic switches and torque motors. During flight, the slow erection circuits are used to maintain verticality. The slow erection rate for both pitch and roll is nominally 2.1°/min.

To prevent spin axis precession during climbs, descents, and turns, the erection circuits can be disabled. The pitch erection is removed when longitudinal accelerations greater than 0.43 m/sec/sec are sensed. This corresponds to a ±2.5° pitch angle. Erection is restored after 3 min or when longitudinal accelerations are lower than the threshold, whichever occurs first.

The threshold for roll erection cutoff is a lateral acceleration of 1.03 m/sec/sec (roll angle of 6°). Roll erection is restored when lateral accelerations drop below the threshold. There were no data available during the tests to monitor the pitch and roll erection circuits.

Pitch error

Ground- The indicated pitch attitude after power as applied to the vertical gyro is shown in figure 4(a). The pitch angle was stabilized by t = 80 sec. The difference between the gyro and INS pitch attitudes was about 0.15° (fig. 4(a)). That error was less than the verticality error specification of ±0.375°.

Flight- During the test flight, pitch attitudes measured by the vertical gyro and the INS are shown in figure 4(b). The corresponding gyro pitch error is plotted in figure 4(b). Prior to turn 1, the acceleration due to takeoff

and to the high pitch attitude caused the pitch erection threshold to be exceeded. The 3-min timer for the pitch erection circuit elapsed by about 170 sec on the plots. During this period, a pitch error of -1.1° was present prior to turn 1. In turn 1, due to a favorable gyro drift, the error decreased to approximately 0.4°. The erection threshold was exceeded again in turn 2. The error increased to -1.2°, where it remained during the approach and landing. The maximum error was -2° during flare.

Roll error

Ground- When power was applied to the vertical gyro, its roll attitude measurement converged rapidly to within 0.4° of the INS roll measurement (fig. 4(c)). A slow, slightly diverging erection is evident to 220 sec when the aircraft started to taxi. At that time, the roll angle was in error about 0.6° compared to the INS. This is larger than the verticality error specification of ±0.375°.

Flight- The roll attitude and attitude error during the flight are shown in figure 4(d). An average roll attitude error of 0.8° is seen before turn 1. In the turn, the roll erection threshold was exceeded. Gimbaling effects caused the roll error to change from 1.5° to -2.5°. After the turn, the erection circuits reduced the error to -1.2°. During turn 2, the gyro roll erection threshold was again exceeded. The roll error changed to an average of about 0.8° where it remained for the duration of the approach.

In right-hand pattern flights (not shown), similar errors were encountered. However, the error peaks in turns were of opposite signs to those in figure 4(d). Overall, the roll attitude error was within ±3°. In the final approaches, the roll attitude error varied from 0° to 1.5°, with a mean error near the static bias of 0.6° seen in figure 4(c). The presence of this bias indicates mounting inaccuracies.

Compass

Description

The compass system used in the Augmentor Wing aircraft is the USAF (United States Air Force) Type J-2 Slaved Gyro Magnetic Compass (Sperry Gyroscope Company's model C-4). A brief description of the general characteristics of this compass system is given below. More details about its operation may be found in reference 6. The compass described is part of the aircraft's instrumentation and is used by, but is not part of, the onboard digital avionics system.

The directional reference is provided by a gyro whose spin axis is horizontal and aligned to the Earth's magnetic meridian. A liquid-level switch operates a torque motor to precess the gyro axis to a local horizontal. The direction-sensing component of the system is a pendulus flux valve unit. This unit detects the horizontal component of the Earth's magnetic field. An electrical signal is then transmitted to the flux valve synchro in the gyro

package. If the gyro is misaligned, it will be precessed until its spin axis is aligned to the Earth's magnetic meridian.

As the aircraft changes direction, the outer case of gyro package rotates in azimuth relative to the gyro axis. The stator of the heading synchro is thus rotated relative to its rotor, providing a signal to control a remotely located visual heading indicator. This synchro signal is also transmitted, via appropriate analog-to-digital conversions, to the digital avionics system to provide a heading reference.

This compass system has error-correction circuits to minimize some magnetic and voltage unbalance effects (one-cycle and two-cycle errors). However, it is subject to several other types of errors for which compensation methods have been devised and used in more recent compass system designs. These errors are described in the following section.

Heading error

Ground- When power is first applied to the compass system, the gyro slaving and leveling rates are boosted above normal. The slaving rate is 60°/min minimum for misalignments greater than 5° and decreases to zero as null is achieved. These rates are sufficient to fully erect the gyro and align its spin axis within 2 to 3 min. This process is seen in figure 5(a). In this case, power was applied at 4 sec. The heading error decreased rapidly to about -5° and then gradually decreased, stabilizing at about 60 sec. Stabilization occurred with an error of about -4.5°.

The probable cause for most of this -4.5° bias is index error. This is due to misalignment of the flux valve and/or synchros with the longitudinal axis of the aircraft. Other secondary errors such as magnetic effects are likely to be present, but no reliable compass-swing calibration data are available for verification.

Flight- As the aircraft flew around the test flightpath, its heading changed as shown in figure 5(b). The compass had errors up to -8° as plotted in figure 5(b). The most predominate errors were the -4.5° bias and the gimbaling error in the turns. The gimbaling error, which is a major source of error in this type compass, occurs because the gyro spin axis is not aligned with the fore-aft or transverse aircraft axis. As the aircraft rolls or pitches, both inner and outer gyro gimbals rotate to keep the spin axis horizontal and pointed in the original direction. Rotation of the outer gimbal causes errors in the indicated heading. This gimbal error can be computed by the equations

$$\tan(\text{actual heading}) = \frac{\tan(\text{indicated heading}) + \tan\theta \sin\phi}{\cos\phi \sec\theta}$$

and

$$\text{gimbal error} = \text{indicated heading} - \text{actual heading}$$

The gimbal error for this flight is shown in figure 5(b). The pitch and roll angles may be seen in figures 4(b) and 4(d), respectively.

Heading error residual after the -4.5° bias and the gimbal errors are removed may be seen in figure 5(b). The predominate errors occurred in and near the turns, being as much as 4°. Two causes of significant errors in turns are real and apparent gyro drift. Real drift is due to internal friction and unbalance. Apparent drift in turns can be caused by (1) the flux valve deviating from the true vertical due to centrifugal acceleration and causing gyro-slaving errors, and (2) the gyro's leveling system reacting to the false vertical, and precessing the spin axis out of the horizontal plane. The effects of these precesses are dependent on the bank angle, nature of the turn, and slaving characteristics. In any case, a component of gyro precession induces errors into the heading indication.

Another source of heading errors is north-turning error. This error occurs in turns from northerly headings in the Northern Hemisphere. In coordinated turns, the pendulus flux valve hangs off from vertical equal to the roll angle. The vertical component of the Earth's magnetic field induces a positive error in turns to the left. This trend is seen in the first part of the turn (figure 5(b)).

As bank angle decreases following turns, the gyro is slaved back to its proper attitude at rates of 1° to 3°/min. This effect is indicated by the decreasing error following the initial turn (fig. 5(b)).

Slaved gyro compass systems are subject to other errors which are generally less significant than those described above. They are minimized in the experimental flights because of the short flight times and distances flown.

Accelerometers

Description

The accelerometer system used in the Augmentor Wing aircraft contains three body-mounted linear accelerometers to provide sensing of aircraft normal, lateral, and longitudinal accelerations. The accelerometers are closed-loop and force-balanced. All accelerometer electronics are contained in each accelerometer. The electronics consist of an electrical pickoff and servo amplifier to electronically provide closed-loop operation. The accelerometer output is a dc signal proportional to acceleration and is used directly by the avionics system's data adapter.

Acceleration errors

As previously described, acceleration outputs from the INS interface are in the form of velocity increments dV, measured over a time interval dt. Conversion of the velocity increment for each axis to the corresponding acceleration is done by dividing dV by dt.

These INS accelerations were then transformed from INS sensing axes to aircraft body axes. The details of the coordinates and transformations are given in appendix B. The body-axis accelerations measured by the strapdown accelerometers contain the gravity vector. The gravity vector was added to

the INS accelerations, using INS Euler angles, so that the INS and strapdown systems measured accelerations can be compared in the body axes.

Ground- The accelerations measured with the aircraft parked on the ramp are shown in figures 6(a)-(c). The lower plot in each figure gives the error in the measured strapdown accelerometer signal as

error = strapdown acceleration - INS acceleration

Small bias errors can be seen in the X and Y accelerations, the lower plots of figures 6(a)-(b). The Z-axis bias is much larger (fig. 6(c). Computed means of the bias are shown in table 2.

Accelerometer outputs are filtered by capacitors, which explains the lower noise level than is seen in the equivalent INS acceleration data (fig. 6(a)).

Flight- Accelerations measured with the aircraft in flight are shown in figures 6(d)-(f). The relatively high X-axis acceleration measured is due primarily to the gravity component at the 10° to 15° pitch attitude prior to turn one, decreasing to 0° at the beginning of turn 2 (fig. 6(d)). The major errors in all three axes occurred during the turns with maximum short-term-mean errors near 0.4 m/sec/sec in the X and Y axes, and about 0.2 m/sec/sec in the Z axis. Mean errors for each axis computed over the whole flight are given in table 3. Errors during stabilized flight between the turns are generally similar to the mean errors for the ground measurements.

Barometric Altimeter

Description

The system implemented for generating the pressure altitude is a vibrating diaphragm, static-pressure sensor. It consists of a rigidly supported metal diaphragm with a vacuum applied to one surface and static pressure from the pitot tube applied to the opposite surface. The diaphragm has a vibrating resonance whose frequency is a direct function of applied static pressure. Conversion of the measured frequency to barometric altitude is done by a table look-up algorithm in the onboard digital computer.

Altitude error

Shown in figure 7 are time histories of the barometric altitude, the altitude as determined by radar, the difference between the two (labeled as Baro altitude error), and the X-radar position. The radar altitude measurement contains a possible error of up to 4 m. The barometric altitude contains a possible error of about 2.7 m, also. This gives rise to a possible total difference between the two measurements of 6.7 m. During level flight the error is within this value. However, during the initial and final portions of flight, the error approaches 10 m. It will be noted that the sign of the error can be correlated with the X-radar time history. That is, the error changes sign in accordance with the sign of the X-radar position.

This type of sign change in the error suggests an unlevel radar reference. Further evidence to support this is contained in previous barometric altimeter error records for similar flightpaths.

CONCLUDING REMARKS

The operation and error characteristics of the avionics system's vertical gyro, compass, accelerometers, and barometric altimeter subsystems have been described. Comparisons were made with equivalent data from an inertial navigation system and a tracking radar system. Tests included data with the STOL aircraft parked on the ramp and during a typical experiment takeoff and approach.

The results indicate that the pitch and roll angles from the vertical gyro had errors up to about 2.5°, primarily in turns. The compass gave heading errors up to -8°, most of which was due to a -4.5° bias. The short level-flight intervals inhibited the ability of the correction circuits in these systems to reduce the maneuver-induced errors. Accelerometer errors as high as 0.2 m/sec/sec (0.02 g) in level flight and up to 0.4 m/sec/sec (0.04 g) in turns were seen, neglecting noise components. Errors in the pitch and roll angles caused errors in acceleration-axis transformations and removal of gravity components. The barometric altitude had errors up to 10 m, but uncertainties in the radar reference could account for part of that error. Avionics systems will be affected by these error characteristics in various ways depending on the flight maneuvers and the system design.

APPENDIX A

SPECIFICATIONS

The known operational characteristics and specifications of the inertial navigation system and the avionics system sensors are documented in this appendix.

Inertial Navigation System

MADE BY: Litton Systems, Inc., Aero Products Division
MODEL NO.: LTN-51

Signal/characteristic	Specification[a]	
Roll		
Range	0° to ±180°	
Index reference	0° = horizon	
Positive direction sense	Right bank	
	Range	
	0° - 30°	30° - 180°
Resolution	0.1°	0.2°
Accuracy	0.5°	1.0°
Signal output	3-wire synchro	
Pitch		
Range	0° to ±180°	
Index reference	0° = horizon	
Positive direction sense	Nose up	
	Range	
	0° - 30°	30° - 180°
Resolution	0.1°	0.2°
Accuracy	0.5°	1.0°
Signal output	3-wire synchro	
True heading		
Range	0° to 360°	
Index reference	0° (north)	
Positive direction sense	Nose right	
Resolution	0.1°	
Accuracy	0.4°	
Signal output	3-wire synchro	

[a]From ARINC characteristics No. 561-5.

True heading (concluded)	
Wander angle[b]	
Range	±180°
Index reference	0° (true north)
Positive direction sense	Nose right
Resolution	Approximately 5 arc-sec
Accuracy	Approximately 0.4°
Signal format	Binary
Delta velocities[c] (50 msec interval)	
Range	±0.98 m/sec
Positive direction sense	
Longitudinal	Forward
Lateral	Right
Normal	Up
Resolution	0.48×10^{-3} m/sec
Accuracy	Approximately 0.48×10^{-3} m/sec
Signal format	Binary

[b] Special output.

[c] Special acceleration outputs through interface.

Vertical Gyro

MADE BY: Sperry Flight Systems
MODEL NO.: VG-321
PART NO.: 2587335-21

Characteristic	Specification
Power input	115 VAC, 400 Hz, 115 VA, 60 W (max start) 115 VAC, 400 Hz, 60 VA, 25 W (max run)
Rotor speed	11,000 rpm (nom.)
Angular momentum	4 million g cm^2/sec
Verticality	±0.375° (level unaccelerated flight)
Erection rates	Roll: fast, 33°/min (nom.) slow, 2.1°/min (nom.) Pitch: fast, 12°/min (nom.) slow, 2.1°/min (nom.)
Erection cut-off threshold	0.10 g lateral = 1 m/sec^2 0.04 g longitudinal = 0.4 m/sec^2
Roll and pitch	3-wire synchro 0.205 VAC/°
Signal outputs	2-wire flight director 0.205 VAC/° 2-wire radar, 0.050 VAC/° 2-wire spare, 0.050 VAC/°
Weight	6.71 kg

Compass

MADE BY: Sperry Gyroscope Co., Division of Sperry Rand Corporation
MODEL NO.: Sperry C-4 (USAF Type J-2)

Characteristic	Specification
Start-up	
Alignment time	3 min
Slaving rates	60°/min when error greater than 5°, decreasing to zero at null
Normal operation	
Gyro	
Power input	115 VAC, 400 Hz
Range	±85° in pitch and roll
Slaving rates	1° - 3°/min when error greater than 5°, decreasing to zero at null
Leveling device	Liquid level switch and torque motor
Signal output	3-wire synchro
Flux valve	
Power input	24 VAC, 400 Hz
Range of pendulosity	±30° in pitch and roll

3-Axis Accelerometer Assembly

MADE BY: Sperry Flight Systems[d]
MFG. PART NO.: 4006992

Characteristic	Specification	
Power input	±15 Vdc, 60 mA per accelerometer	
	Normal	Lateral/Longitudinal
Range	-1 to +4 g	0 ± 1 g
Scale factor (100 K external load)	2 VAC/g (0 V @ +1 g)	5 Vdc/g
Scale factor tolerance @ 25°C	±0.25%	±0.25%
Null @ 25°C	0.015 g	0.0016 g
Scale factor change with temperature	±0.018%/°C	±0.018%/°C
Null change with temperature	±0.0006 g/°C	±0.0006 g/°C
Hysteresis	±0.0008 g	±0.0002 g
Cross axis sensitivity	±0.002 g/g	±0.002 g/g
Natural frequency	> 50 Hz	> 50 Hz
Case alignment	±0.25°	±0.25°
Weight	0.48 kg for complete assembly	
Positive direction sense	upward	right/forward

[d] Assembly contains three accelerometers manufactured by Systron Donner: Normal = model 4384A-4-P5, Sperry part no. 4010677-1; Lateral/Longitudinal = model 4384A-1-P6, Sperry part no. 4010677-2.

Static Pressure Sensor
(Barometric Altimeter)

MADE BY: Sperry Flight Systems
MODEL NO.: None
PART NO.: 4009996

Characteristic	Specification
Power input	+15 Vdc, 400 mA -15 Vdc, 50 mA
Range	0 to 35 in. Hg
Overpressure limit	150% of normal range
Output range	1 to 4 kHz
Resolution	Better than 0.0001 in. Hg
Accuracy	0.003 in. Hg + 0.02% of pressure in in. Hg with output frequency corrected for sensor temperature
Hysteresis	Less than 0.003 in. Hg
Temperature	Linear from 0.0006 in. Hg/C at 30 in. Hg to zero in. Hg/C at 1.0 in. Hg. (Constant 0.0002/C times reading in in. Hg.)
g-sensitivity	0.010 in. Hg/g acceleration (normal axis of diaphragm) 0.001 in. Hg/g acceleration (tangent axis of diaphragm)
Temperature sensor output voltage as function of T	Typical - linear over range
Weight	1.22 kg

APPENDIX B

INS COORDINATE TRANSFORMATIONS

Define the coordinate systems of interest (figure 8).

(1) Orientation of runway axes with respect to north, east, and down

$$\begin{pmatrix} \bar{R}_1 \\ \bar{R}_2 \\ \bar{R}_3 \end{pmatrix} = \begin{pmatrix} C\psi_{R/N} & S\psi_{R/N} & C \\ -S\psi_{R/N} & C\psi_{R/N} & 0 \\ 0 & 0 & 1 \end{pmatrix} \begin{pmatrix} \bar{N} \\ \bar{E} \\ \bar{D} \end{pmatrix}$$

where sine and cosine are represented by S and C, respectively.

(2) Orientation of INS-marked axes with respect to north, east, and down

$$\begin{pmatrix} \bar{P}_1 \\ \bar{P}_2 \\ \bar{P}_3 \end{pmatrix} = \begin{pmatrix} C\psi_w & S\psi_w & 0 \\ -S\psi_w & C\psi_w & 0 \\ 0 & 0 & 1 \end{pmatrix} \begin{pmatrix} \bar{N} \\ \bar{E} \\ \bar{D} \end{pmatrix}$$

where ψ_w is the INS wander angle.

(3) Orientation of INS-sensing axes with respect to INS marked axes

$$\begin{pmatrix} \bar{S}_1 \\ \bar{S}_2 \\ \bar{S}_3 \end{pmatrix} = \begin{pmatrix} 1 & 0 & 0 \\ 0 & 1 & 0 \\ 0 & 0 & -1 \end{pmatrix} \begin{pmatrix} \bar{P}_1 \\ \bar{P}_2 \\ \bar{P}_3 \end{pmatrix}$$

(4) Orientation of vehicle body axes with respect to north, east, and down using INS Euler Angles

$$\begin{pmatrix} \bar{b}_1 \\ \bar{b}_2 \\ \bar{b}_3 \end{pmatrix} = \begin{pmatrix} 1 & 0 & 0 \\ 0 & C\phi & S\phi \\ 0 & -S\phi & C\phi \end{pmatrix} \begin{pmatrix} C\theta & 0 & -S\theta \\ 0 & 1 & 0 \\ S\theta & 0 & C\theta \end{pmatrix} \begin{pmatrix} C\psi & S\psi & 0 \\ -S\psi & C\psi & 0 \\ 0 & 0 & 1 \end{pmatrix} \begin{pmatrix} \bar{N} \\ \bar{E} \\ \bar{D} \end{pmatrix}$$

Using the above transformations we can obtain the values of accelerations in the coordinate systems of interest.

(1) Transform INS-sensing axis accelerations to runway axes

$$\begin{pmatrix} A_{R_1} \\ A_{R_2} \\ A_{R_3} \end{pmatrix} = \begin{pmatrix} C\psi_{S/R} & S\psi_{S/R} & 0 \\ -S\psi_{S/R} & C\psi_{S/R} & 0 \\ 0 & 0 & -1 \end{pmatrix} \begin{pmatrix} A_{S_1} \\ A_{S_2} \\ A_{S_3} \end{pmatrix}$$

where $\psi_{S/R} = \psi_{R/N} - \psi_w$.

(2) Transform runway axes accelerations into aircraft body axes

$$\begin{pmatrix} A_{b_1} \\ A_{b_2} \\ A_{b_3} \end{pmatrix} = \begin{pmatrix} C\theta C\psi_E & C\theta S\psi_E & -S\theta \\ S\phi S\theta C\psi_E - C\phi S\psi_E & S\phi S\theta S\psi_E + C\phi C\psi_E & S\phi C\theta \\ C\phi S\theta C\psi_E + S\phi S\psi_E & C\phi S\theta S\psi_E - S\phi C\psi_E & C\phi C\theta \end{pmatrix} \begin{pmatrix} A_{R_1} \\ A_{R_2} \\ A_{R_3} \end{pmatrix}$$

where $\psi_E = \psi - \psi_{R/N}$.

REFERENCES

1. Pallett, E. H. J.: Aircraft Instruments, Principles and Applications. Pitman Publishing Corp., 1972.

2. Neuman, F.; and Warner, D. N., Jr.: A STOL Terminal Area Navigation System. NASA TM X-62,348, 1974.

3. Thibodeau, Jerry J.: Effect of Gyro Vertically Error on Lateral Autoland Tracking Performance for an Inertially Smoothed Control Law. NASA TM X-3545, 1977.

4. Air Transport Inertial Navigation System - INS. ARINC Characteristic no. 561-5, 1969.

5. Warner, D. N., Jr.; and Moran, F. J.: Flight Test Evaluation Errors in the MODILS and TACAN Navigation Aids at NALF Crows Landing. NASA TM-78584, 1979.

6. Handbook, Operation and Service Instructions, Type J-2 Slaved Gyro Magnetic Compass System. USAF T.O. 5N1-2-4-1, 1954.

TABLE 1.- RADAR ACCURACY (2σ)

Long range	
Azimuth	0.6 mrad
Elevation	0.6 mrad
Range	4.3 m, range < 3050 m 4.3 m + 10^{-3} (R-3050), range > 3050 m

Near touchdown (on STOLport)		
	-600 m < X < 0	0 < X < 300 m
X	3.7 m	3.1 m
Y	1.2 m	3.1 m
Z	1.2 m	1.2 m

TABLE 2.- ACCELERATION ERRORS FOR AIRCRAFT ON THE GROUND

Axis	Mean bias (m/sec/sec)
X	0.015
Y	-.005
Z	-.063

TABLE 3.- ACCELERATION ERRORS FOR THE AIRCRAFT IN FLIGHT

Axis	Mean bias (m/sec/sec)
X	-0.021
Y	-.017
Z	-.057

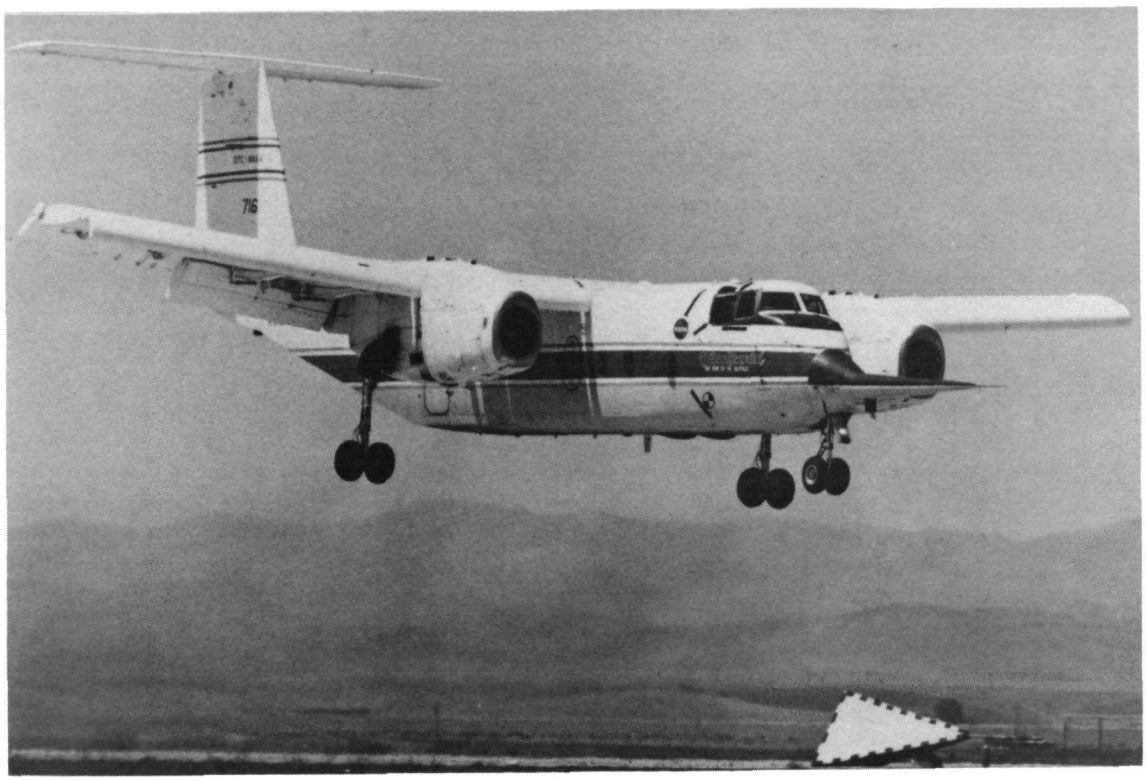

Figure 1.- Augmentor wing jet STOL research aircraft.

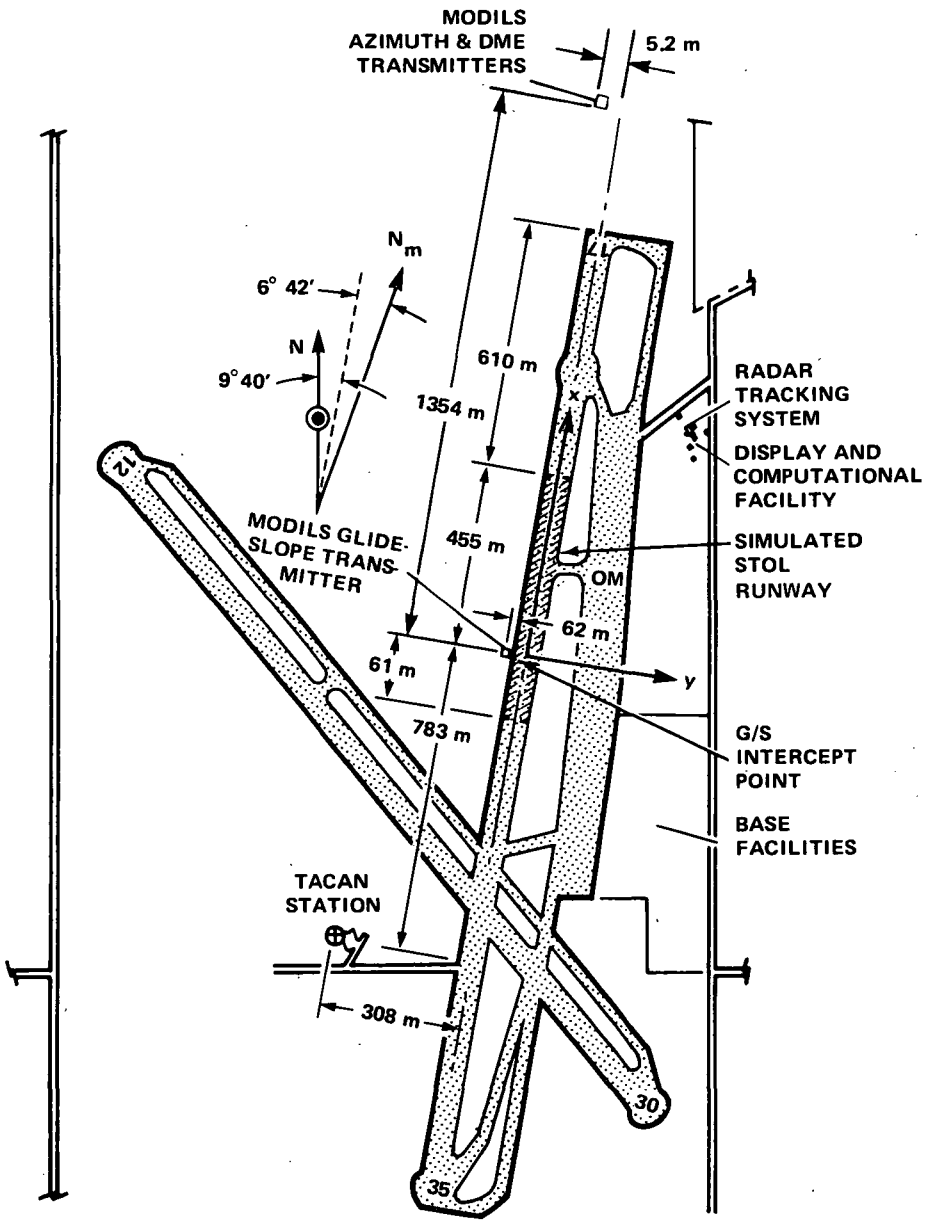

Figure 2.- Ground support equipment deployment at Crows Landing.

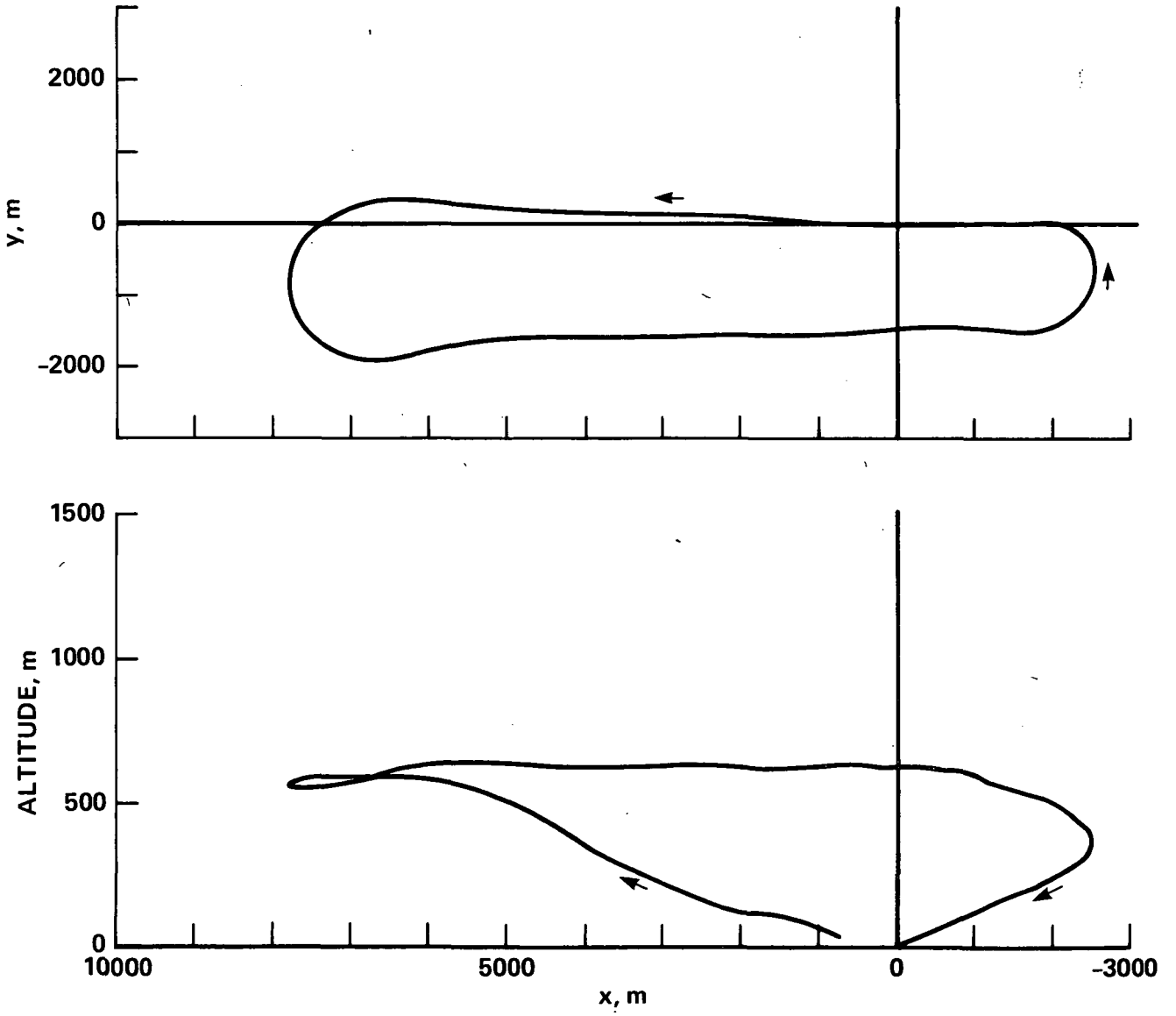

(a) Horizontal and vertical as a function of X

Figure 3.- Aircraft flightpath.

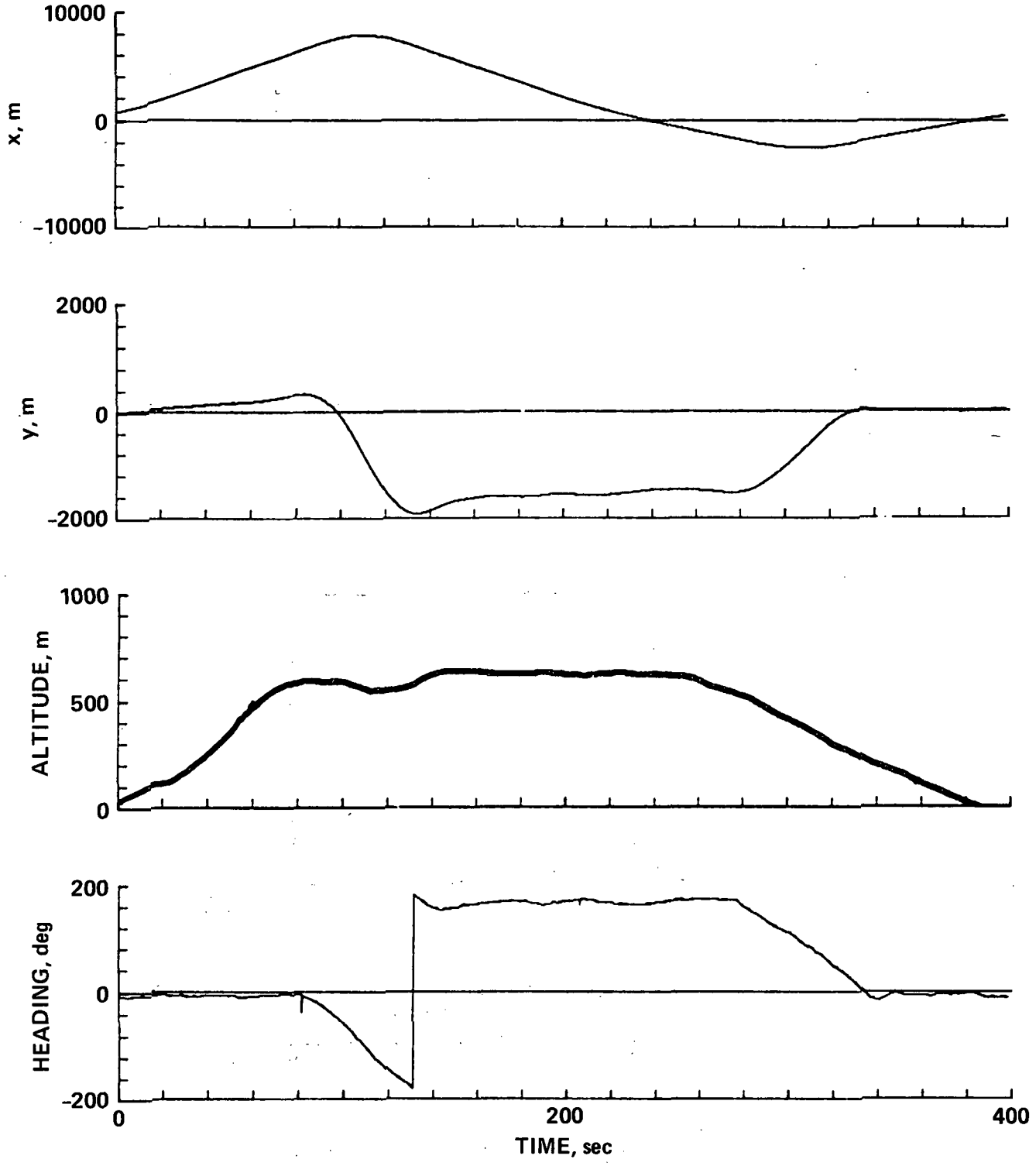

(b) Function of time.

Figure 3.- Concluded.

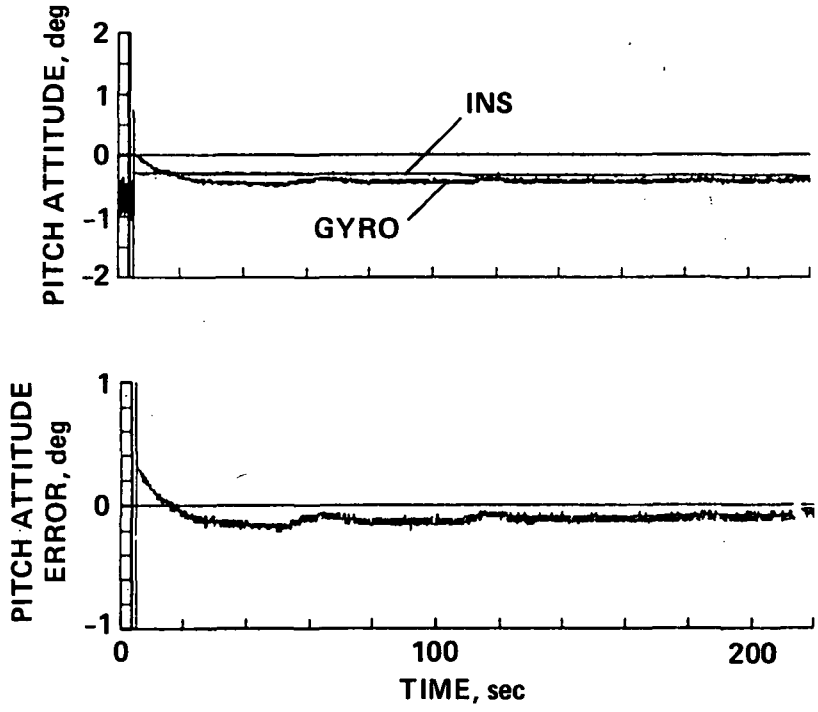

(a) Pitch attitude, error on ground.

Figure 4.- Continued.

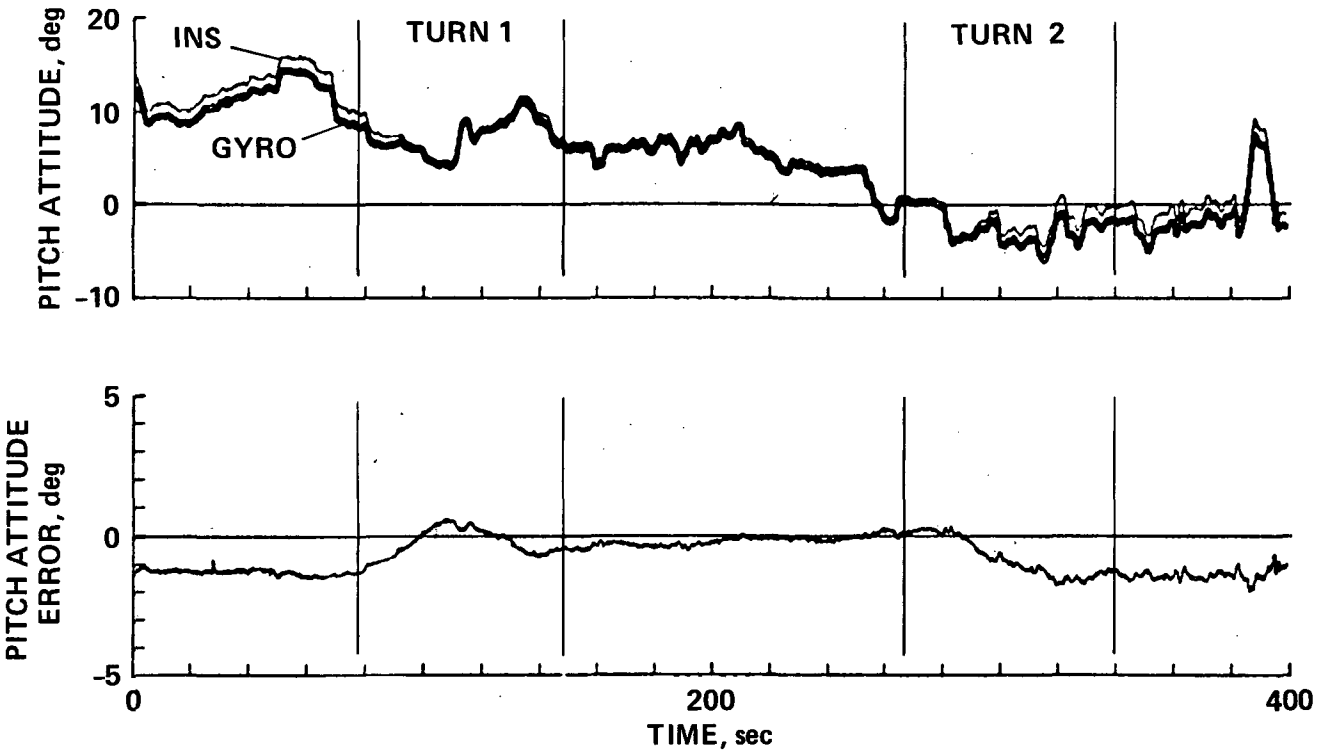

(b) Pitch attitude; error in flight.

Figure 4.- Continued.

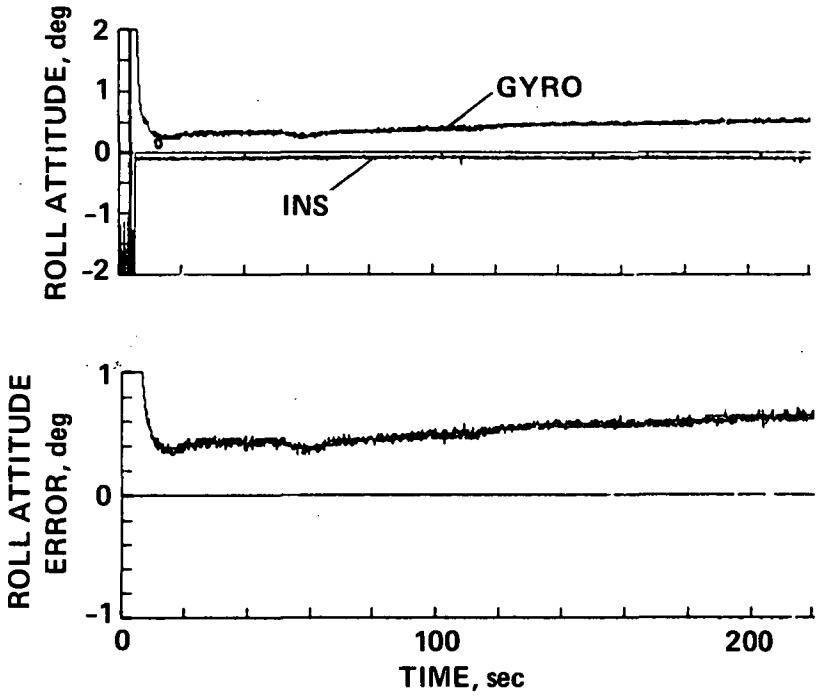

(c) Roll attitude; error on ground.

Figure 4.- Continued.

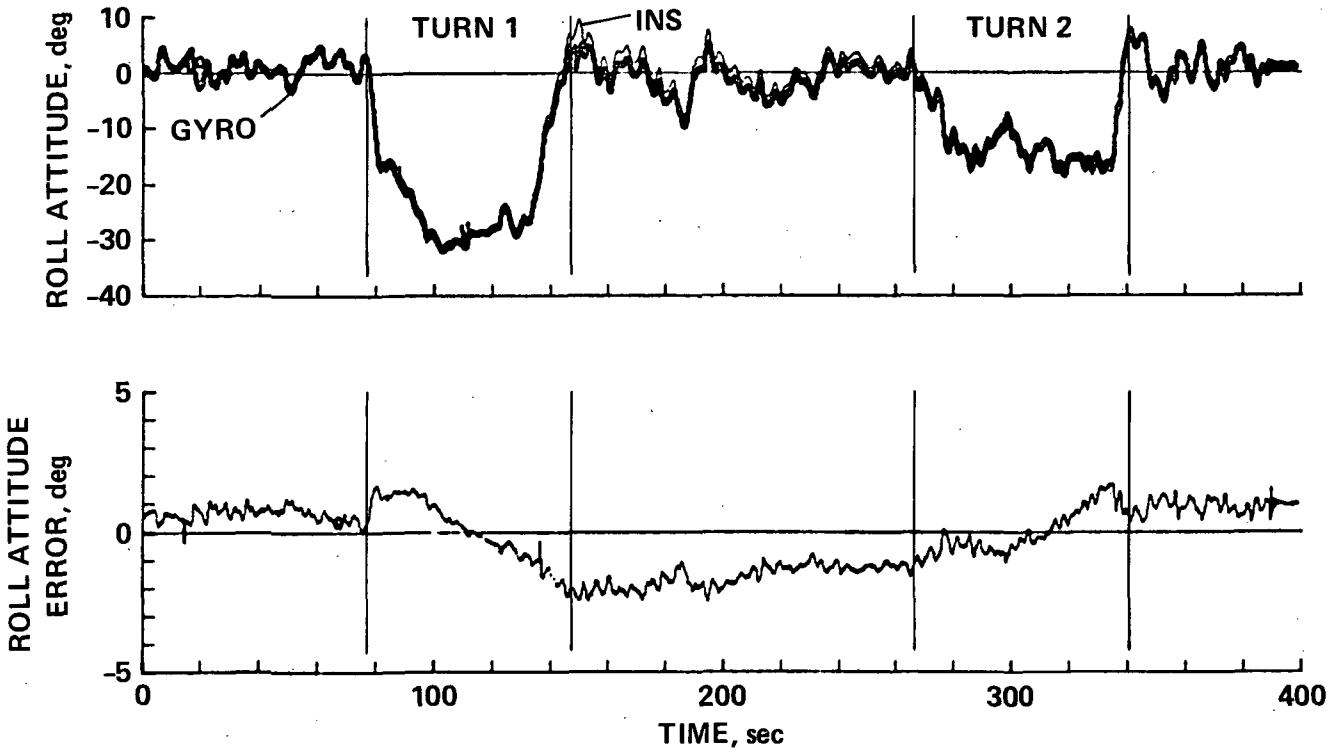

(d) Roll attitude; error in flight.

Figure 4.- Concluded.

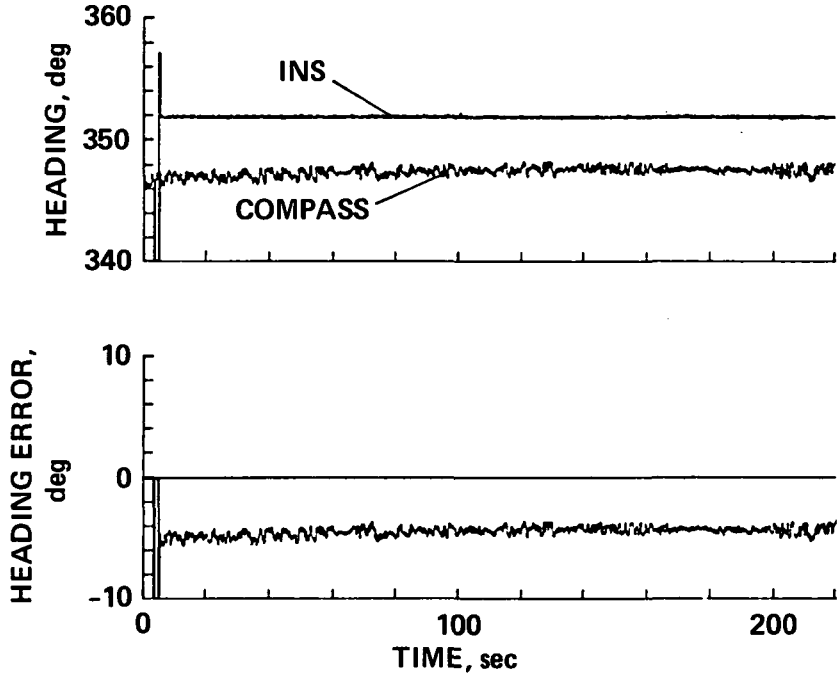

(a) Errors on ground.

Figure 5.- Compass heading.

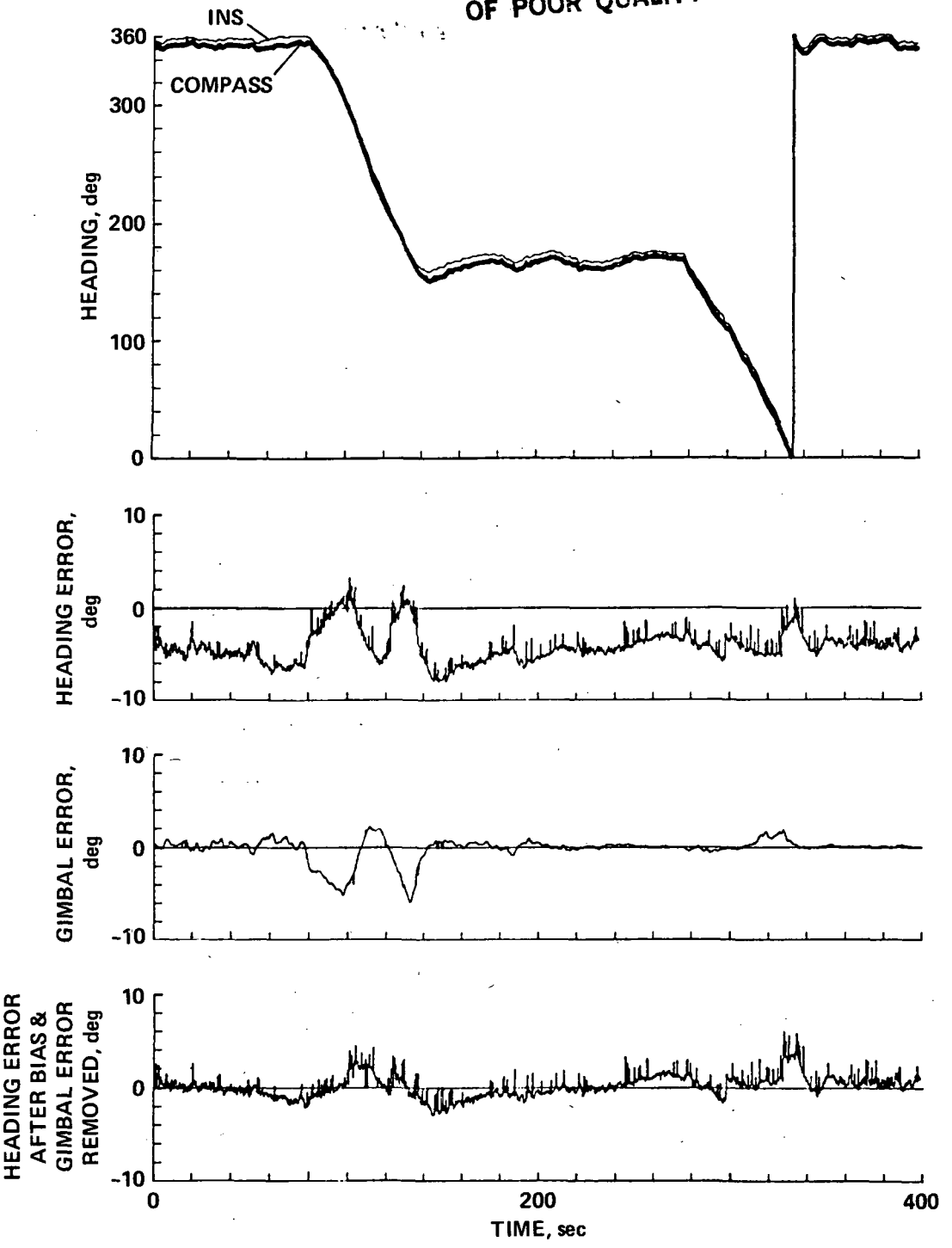

(b) Errors in flight.

Figure 5.- Concluded.

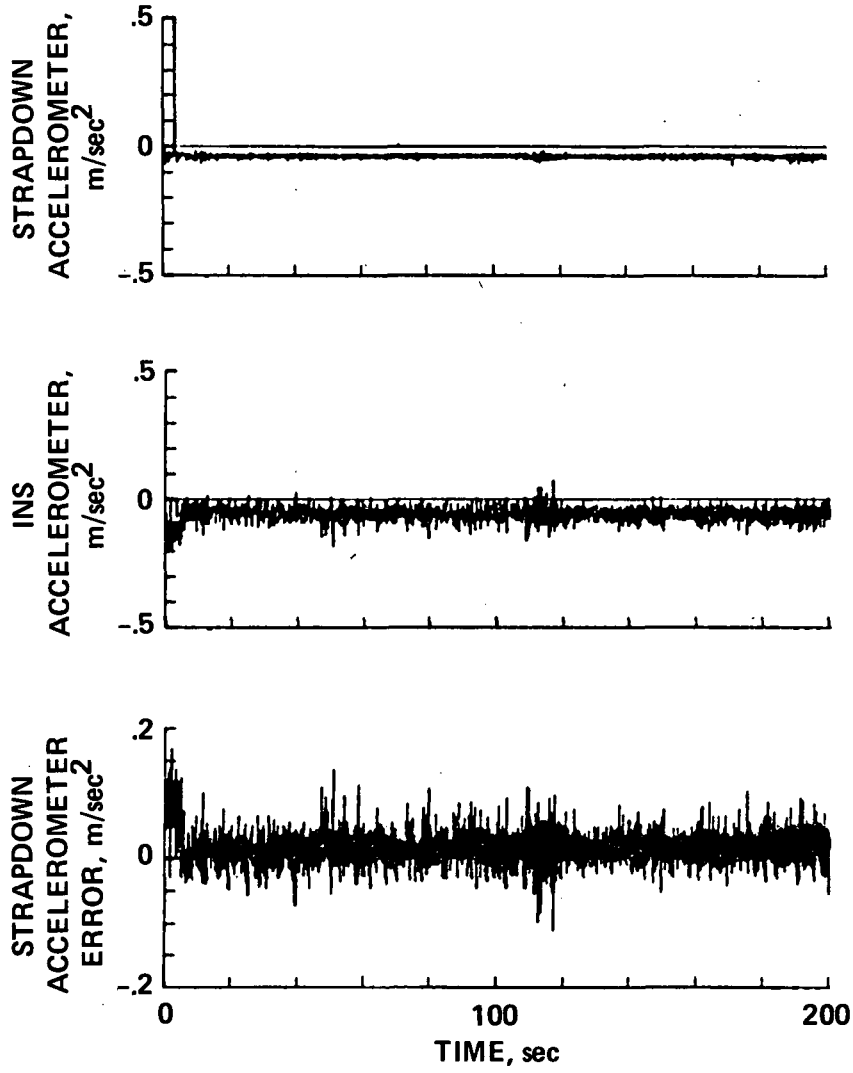

(a) X-body; aircraft on ground.

Figure 6.- Accelerations.

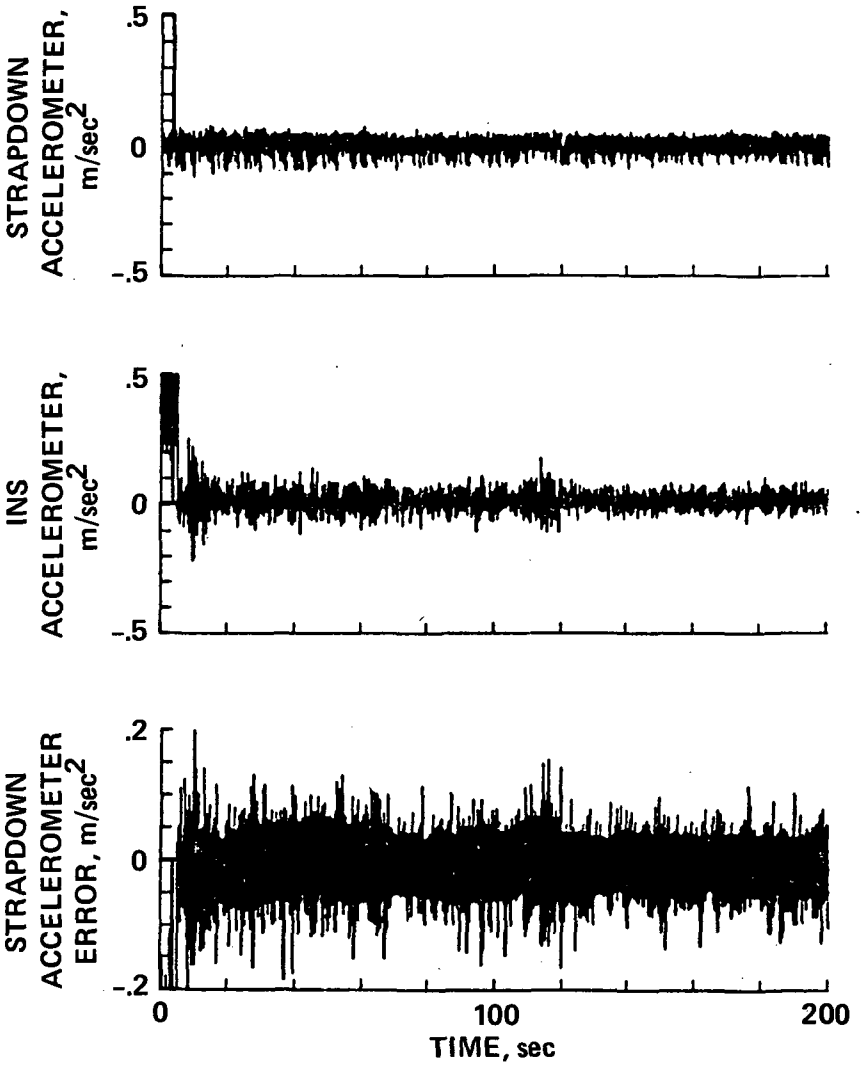

(b) Y-body; aircraft on ground.

Figure 6.- Continued.

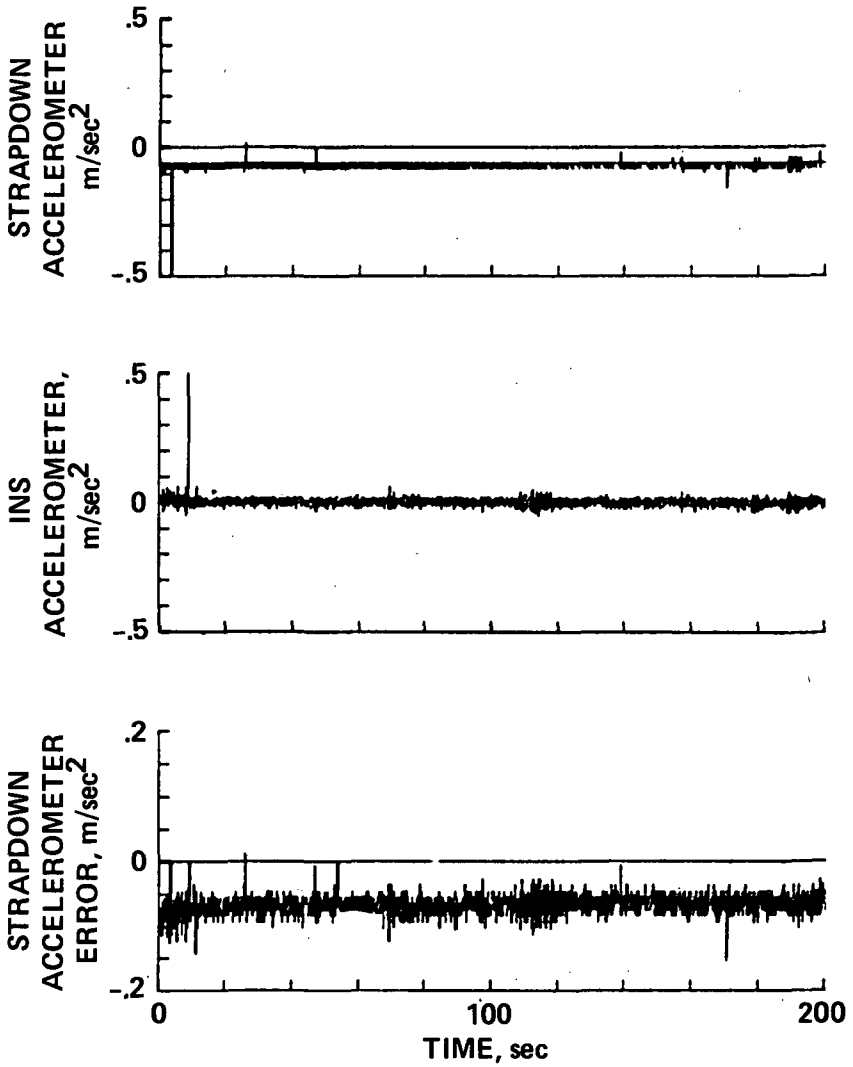

(c) Z-body; aircraft on ground.

Figure 6.- Continued.

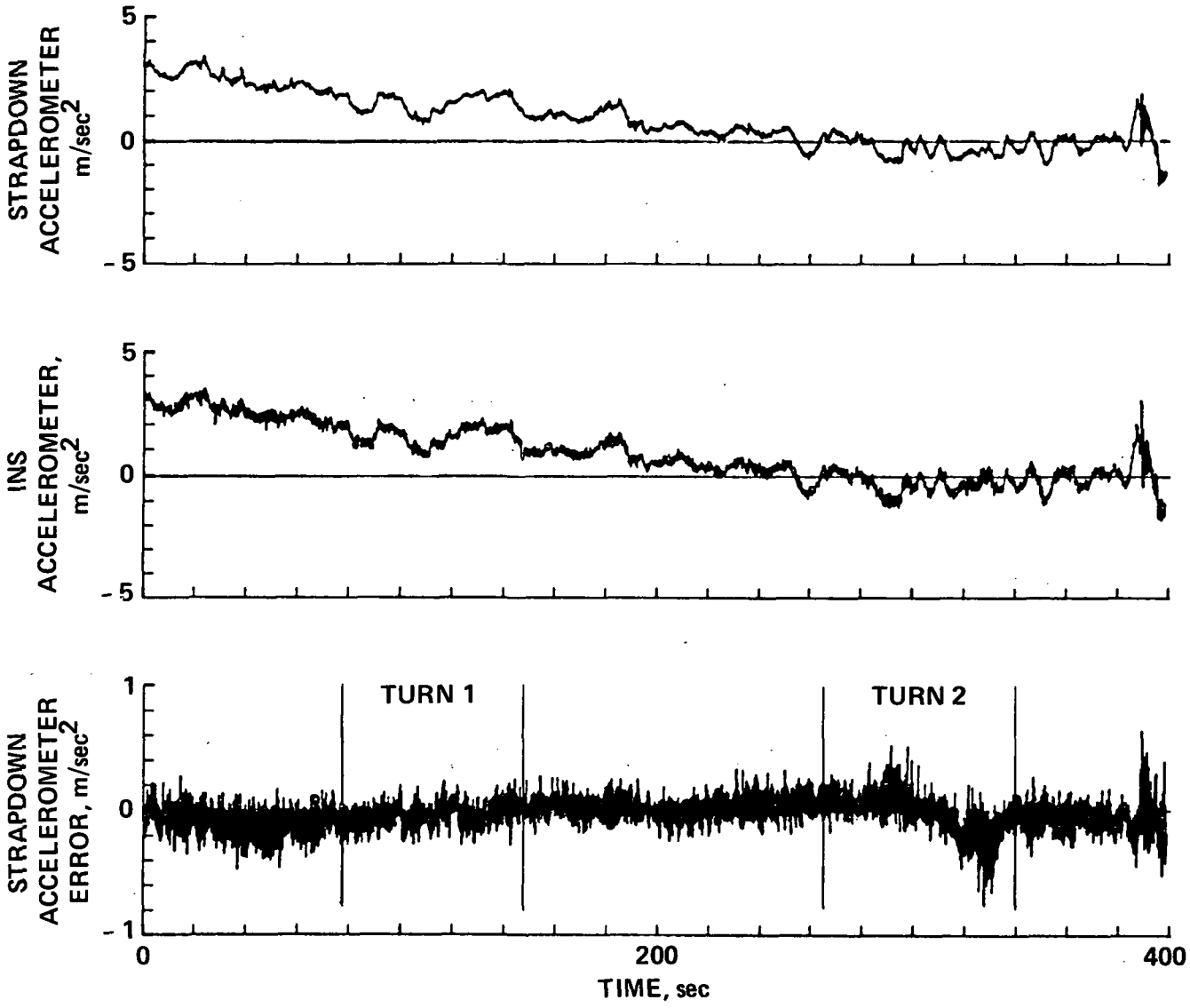

(d) X-body; aircraft in flight.

Figure 6.- Continued.

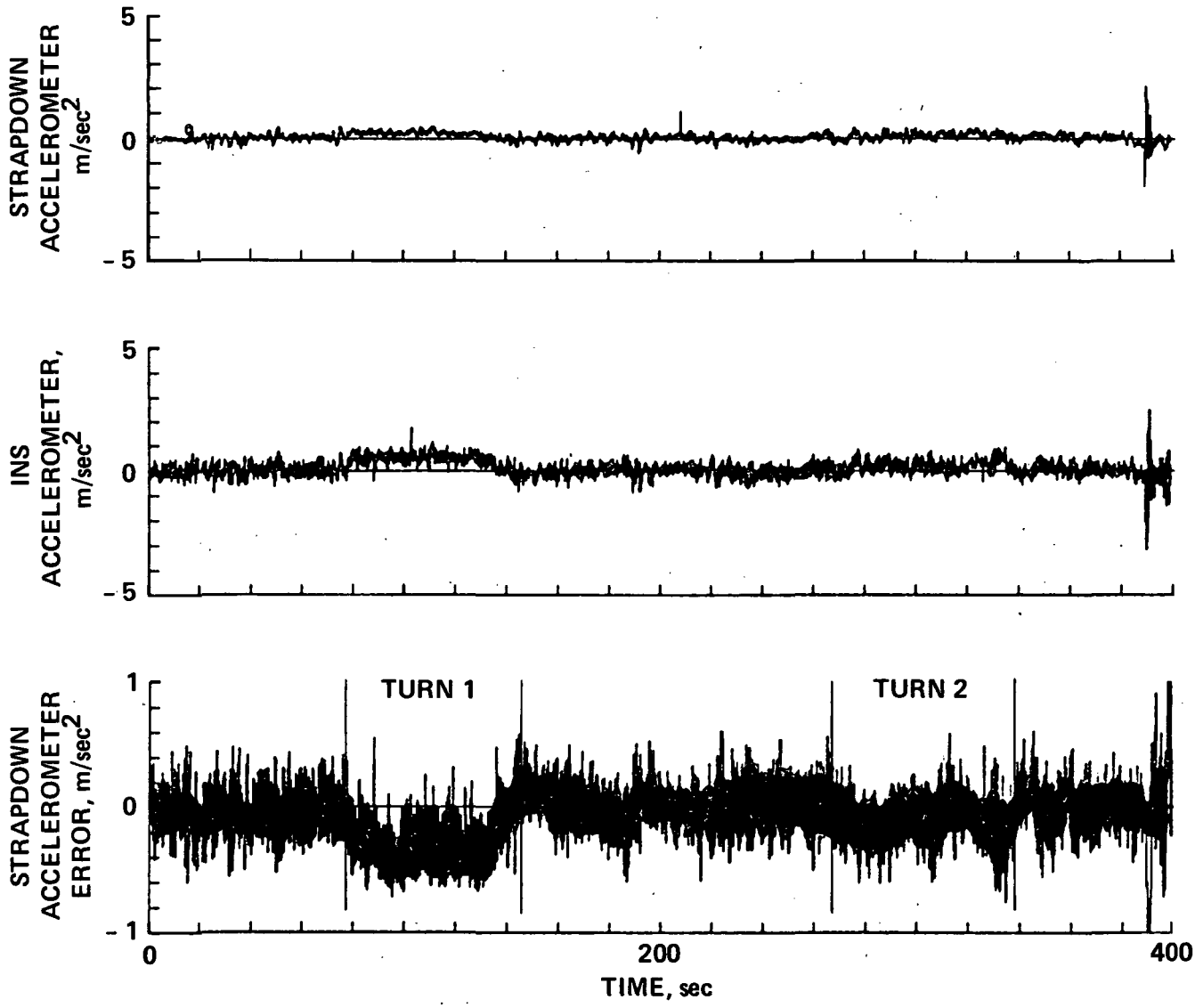

(e) Y-body; aircraft in flight.

Figure 6.- Continued.

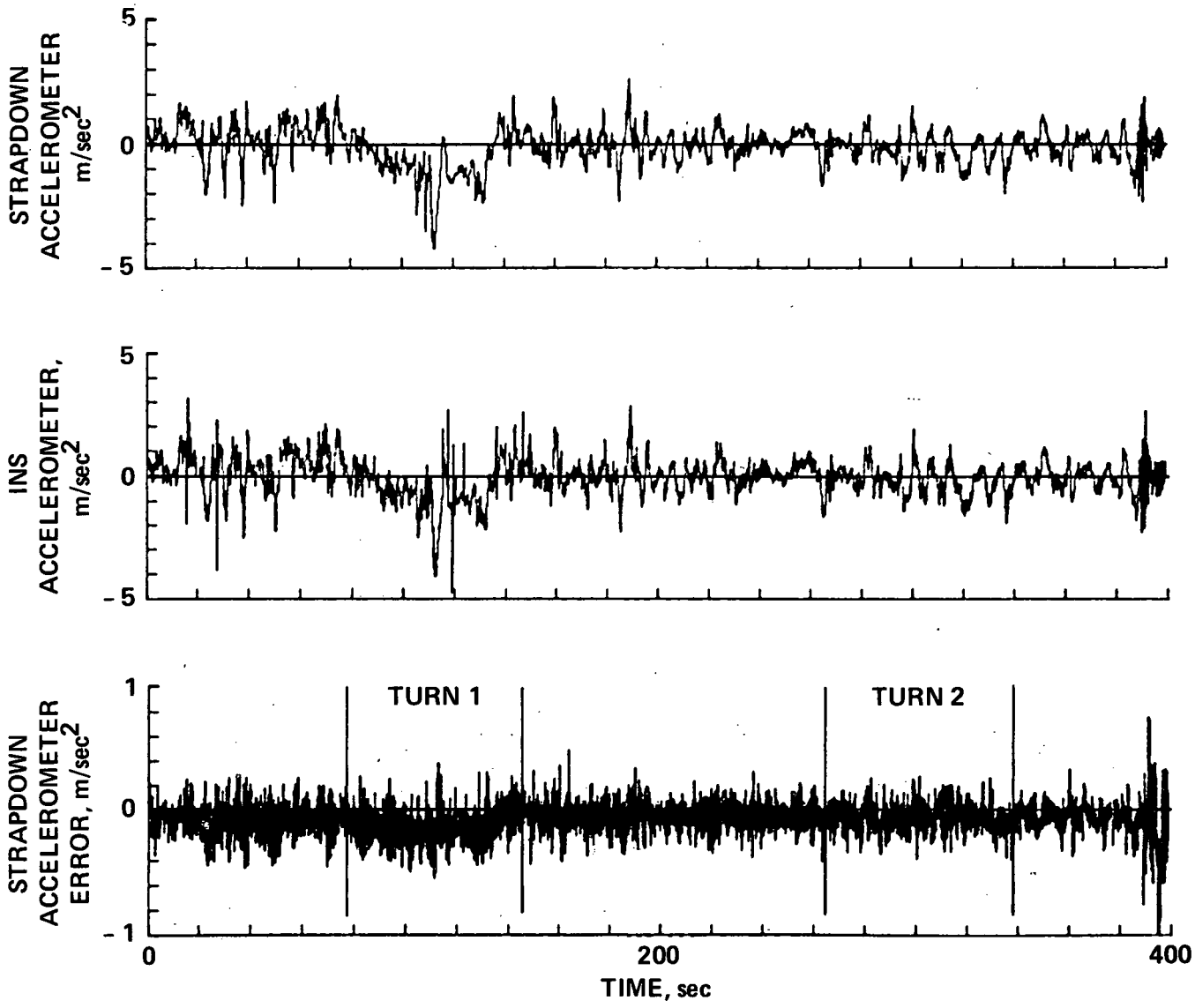

(f) Z-body; aircraft in flight.

Figure 6.- Concluded.

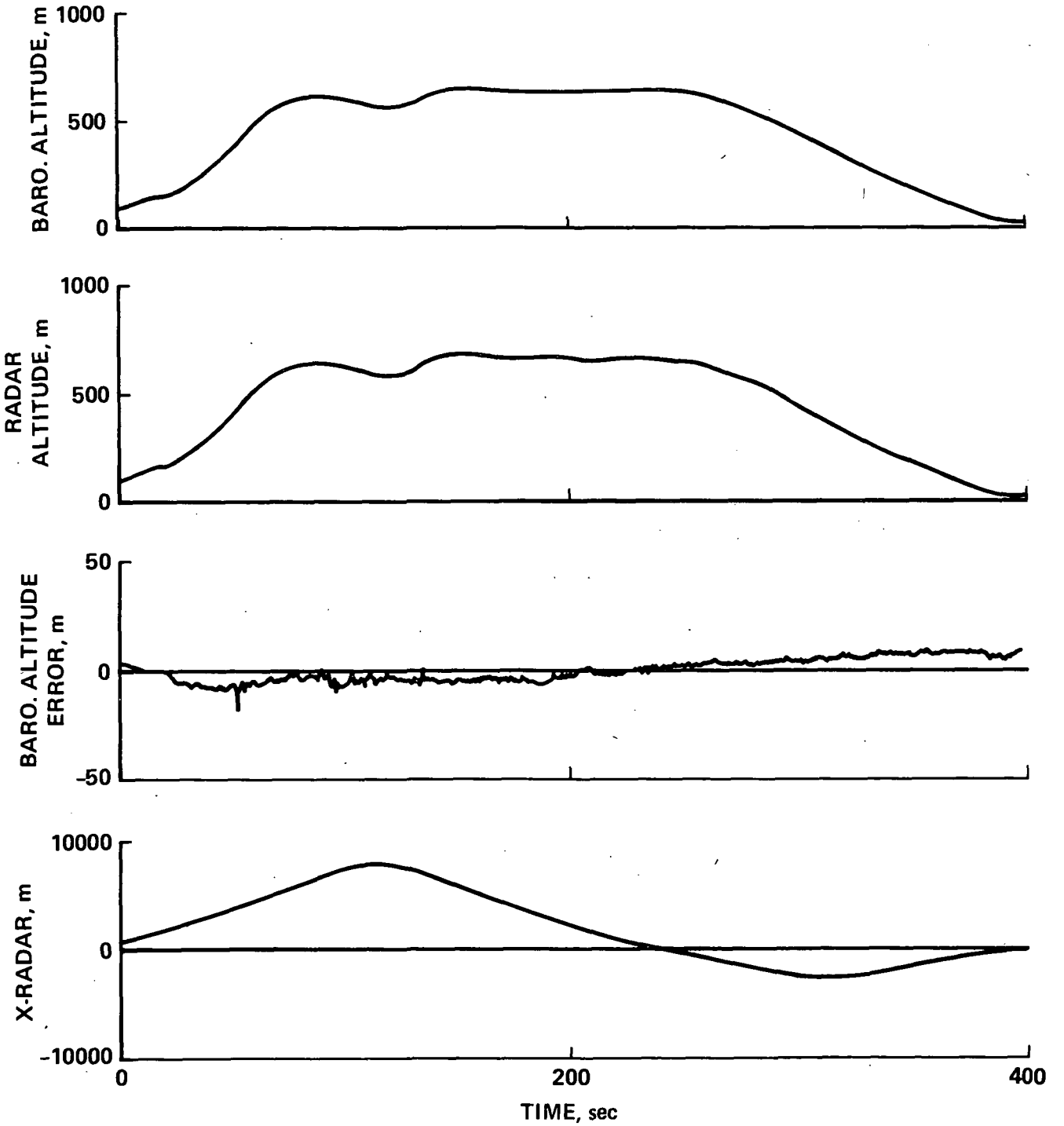

Figure 7.- Comparison of barometric altimeter with radar measurement.

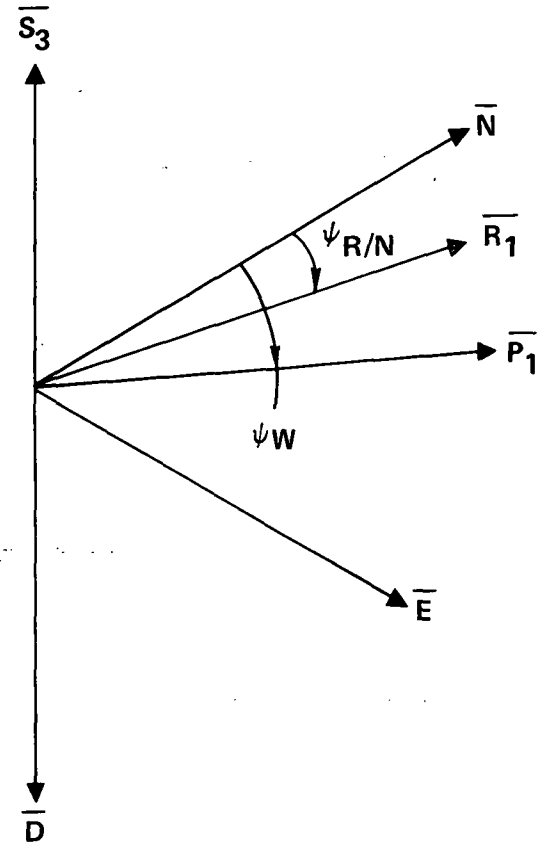

Figure 8.- Diagram of coordinate systems.

1. Report No.	2. Government Accession No.	3. Recipient's Catalog No.
NASA TM-81154		

4. Title and Subtitle	5. Report Date
FLIGHT TEST OF NAVIGATION AND GUIDANCE SENSOR ERRORS MEASURED ON STOL APPROACHES	6. Performing Organization Code

7. Author(s)	8. Performing Organization Report No.
David N. Warner, Jr. and F. J. Moran	A-8008
	10. Work Unit No. 532-02-01
9. Performing Organization Name and Address	11. Contract or Grant No.
Ames Research Center, NASA Moffett Field, Calif. 94035	
	13. Type of Report and Period Covered
12. Sponsoring Agency Name and Address	Technical Memorandum
National Aeronautics and Space Administration Washington, D.C. 20546	14. Sponsoring Agency Code

15. Supplementary Notes

16. Abstract

Navigation and guidance sensor error characteristics have been measured during STOL approach-flight investigations. Data from some of the state sensors of a digital avionics system have been compared to corresponding outputs from an inertial navigation system. These sensors include the vertical gyro, compass, and accelerometers. Barometric altimeter data were compared to altitude measured by a tracking radar. Data were recorded with the Augmentor Wing Jet STOL Research Aircraft parked and in flight.

17. Key Words (Suggested by Author(s))	18. Distribution Statement
Aircraft Instrumentation	Available from originating office only STAR Category - 06

19. Security Classif. (of this report)	20. Security Classif. (of this page)	21. No. of Pages	22. Price*
Unclassified	Unclassified	43	

*For sale by the National Technical Information Service, Springfield, Virginia 22161